Significant Findings: Seasonal Distributions of Global Ocean Chlorophyll and Nutrients with a Coupled Ocean General Circulation, Biogeochemical, and Radiative Model. II. Comparisons with Satellite and *In situ* Data

Watson W. Gregg

Submitted to Journal of Geophysical Research 2000

A coupled ocean general circulation, biogeochemical, and radiative model was constructed to evaluate and understand the nature of seasonal variability of chlorophyll and nutrients in the global oceans. Biogeochemical processes in the model were determined from the influences of circulation and turbulence dynamics, irradiance availability, and the interactions among three functional phytoplankton groups (diatoms, chlorophytes, and picoplankton) and three nutrients (nitrate, ammonium, and silicate).

Basin scale (>1000 km) model chlorophyll seasonal distributions were statistically positively correlated with CZCS chlorophyll in 10 of 12 major oceanographic regions, and with SeaWiFS in all 12. Notable disparities in magnitudes occurred, however, in the tropical Pacific, the spring/summer bloom in the Antarctic, autumn in the northern high latitudes, and during the southwest monsoon in the North Indian Ocean. Synoptic scale (100-1000 km) comparisons of satellite and *in situ* data exhibited broad agreement, although occasional departures were apparent. Model nitrate distributions agreed with *in situ* data, including seasonal dynamics, except for the equatorial Atlantic. The overall agreement of the model with satellite and *in situ* data sources indicated that the model dynamics offer a reasonably realistic simulation of phytoplankton and nutrient dynamics on basin and synoptic scales.

Science Priorities: Seasonal Distributions of Global Ocean Chlorophyll and Nutrients with a Coupled Ocean General Circulation, Biogeochemical, and Radiative Model. II. Comparisons with Satellite and *In situ* Data

Watson W. Gregg

Submitted to Journal of Geophysical Research 2000

Priority#1 Land Cover Change and Global Productivity

Seasonal Distributions of Global Ocean Chlorophyll and Nutrients with a Coupled Ocean General Circulation, Biogeochemical, and Radiative Model. II. Comparisons with Satellite and *In situ* Data

Watson W. Gregg

Laboratory for Hydrospheric Processes, NASA/ Goddard Space Flight Center

Abstract. A coupled ocean general circulation, biogeochemical, and radiative model was constructed to evaluate and understand the nature of seasonal variability of chlorophyll and nutrients in the global oceans. Biogeochemical processes in the model were determined from the influences of circulation and turbulence dynamics, irradiance availability, and the interactions among three functional phytoplankton groups (diatoms, chlorophytes, and picoplankton) and three nutrients (nitrate, ammonium, and silicate).

Basin scale (>1000 km) model chlorophyll seasonal distributions were statistically positively correlated with CZCS chlorophyll in 10 of 12 major oceanographic regions, and with SeaWiFS in all 12. Notable disparities in magnitudes occurred, however, in the tropical Pacific, the spring/summer bloom in the Antarctic, autumn in the northern high latitudes, and during the southwest monsoon in the North Indian Ocean. Synoptic scale (100-1000 km) comparisons of satellite and *in situ* data exhibited broad agreement, although occasional departures were apparent. Model nitrate distributions agreed with *in situ* data except for the equatorial Atlantic. The overall agreement of the model with satellite and *in situ* data sources indicated that the model dynamics offer a reasonably realistic simulation of global phytoplankton and nutrient dynamics on basin and synoptic scales.

The success of the model was attributed to the application of a generalized, processes-driven approach as opposed to regional parameterization, and the existence of multiple phytoplankton groups with different physiological and physical properties. These factors enabled the model to simultaneously represent many aspects of the great diversity of physical, biological, chemical, and radiative environments encountered in the global oceans.

1. Introduction

In a companion paper [*Gregg*, 2000], a coupled physical/biogeochemical/radiative model was developed to facilitate understanding of the dynamical processes and interactions affecting the seasonal distributions of global ocean chlorophyll and nutrients. In that effort, results focused on the seasonal distributions of three phytoplankton functional groups contained in the model: diatoms, chlorophytes (simulating flagellates), and picoplankton (primarily cyanobacteria but also including prochlorophytes). Different responses to seasonal forcing were clearly shown by the different groups, that in general conformed to the limited set of observations available.

In this paper, the seasonal distributions of total chlorophyll (the sum of the three phytoplankton groups) and nutrients are compared with the more extensive data sets available. These include remote sensing observations of chlorophyll from the Coastal Zone Color Scanner (CZCS) and the Sea-Viewing Wide Field-of-view Sensor (SeaWiFS), and the extensive archives of seasonal chlorophyll and nutrients from the NOAA/National Oceanographic Data Center (NODC)/Ocean Climate Laboratory (OCL). The focus here is on the surface layer only, because of the availability of remote sensing and *in situ* data for validation.

2. Methods

Comparisons of the model with satellite and *in situ* data are basin scale (> 1000 km), which are used to evaluate the overall performance of the model, and direct image-to-image comparisons which are used to evaluate synoptic scale (100-1000km) aspects of the model. Regions are defined as in *Conkright et al.* [1998a, 1994]: Antarctic is defined as southward of –40° latitude, the North Pacific and Atlantic Oceans are northward of 40°, and equatorial regions are bounded by –10° and 10°.

CZCS monthly climatological pigment data were obtained from the NASA/Goddard Space Flight Center Distributed Active Archive Center (GSFC-DAAC). This data set can be considered to represent a climatology because of the length of data collection (1978-1986). CZCS pigments were converted to chlorophyll using *O'Reilly et al.* [1998] for the basin-scale comparisons, but were left as pigments for the synoptic scale (imagery) analyses.

SeaWiFS data were also obtained from the NASA/GSFC-DAAC. Unfortunately, SeaWiFS data available prior to June 2000 appeared to overestimate chlorophyll concentrations [*Conkright and Gregg,* 2000] as compared to other data sets, such as the CZCS, the NOAA/NODC/OCL *in situ* archive, and a blended analysis using *in situ* data and the CZCS archive [*Gregg and Conkright,* 2000]. This was attributed to 1) errors associated with the assumption that water-leaving radiances at the near-infrared (NIR) bands of SeaWiFS are negligible, and 2) bio-optical algorithm. An excessively large number of maximum chlorophyll concentrations (64 mg m^{-3}) were produced by the SeaWiFS processing algorithms, that appeared to bias the global means [*Conkright and Gregg,* 2000].

SeaWiFS Level-1A Global Area Coverage (GAC) data (4-km resolution) were obtained from the GSFC-DAAC. The SeaWiFS September 1997 to February 2000 archive was re-analyzed using standard methods for calibration [NASA SeaWiFS Project Table 199902] and atmospheric correction [*Gordon and Wang*, 1994]. Modifications were made to 1) iteratively estimate water-leaving radiance contributions to the NIR bands using *Siegel et al.* [2000], 2) apply the OC3 bio-optical algorithm [*O'Reilly et al.*, 1998], which utilizes the ratio of 443 nm to 555 nm, and switches to a 510 nm to 555 nm ratio when the radiance at 510 nm exceeds that at 443 nm. Additional modifications included the application of spectral foam reflectance [*Frouin et al.*, 1996], elimination of data when the solar zenith angle exceeded 70°, elimination of all chlorophyll values > 25 mg m^{-3}, and exclusion of data when the aerosol reflectance at 865 nm exceeded 0.02. This latter modification avoids excessive sun glint and optically thick aerosols, both of which produce inaccurate chlorophyll derivations.

These modifications appear to ameliorate the adverse effects on chlorophyll contained in the original processing effort. Re-analyzed SeaWiFS chlorophyll concentrations (Figure 1) show a major reduction in global mean value compared to other comparable data sets, and more importantly, a reduction in the variance. This reduction in variance is especially indicative of an improvement since it is now in agreement with the CZCS and blended data sets. NIR, bio-optical algorithm, and spectral foam reflectance modifications were included in the re-processing of SeaWiFS data initiated in May 2000 by the SeaWiFS Project [C.R. McClain, NASA SeaWiFS Project, personal communication, 2000].

Seasonal chlorophyll and nitrate climatologies were obtained from NODC/OCL archives [*Conkright et al.*, 1998b; 1998c; 1998d]. Comparisons were also made between the model outputs and these data sets.

3. Results

3.1 Seasonal Trends in Chlorophyll: Basin Scale Comparisons with CZCS

Basin mean chlorophyll values computed from the model after 4 years from initialization exhibit a wide range of responses, from elevated values in the high latitudes (North Pacific and Atlantic, and Antarctic), to low values in the mid-latitudes, to moderate values in the tropics (Figure 2). These basin ranges in chlorophyll concentrations are in agreement with the CZCS. Seasonal variability also exhibits different responses seasonally: from a large dynamic range in the high latitudes, to moderate variability in the mid-latitudes, to little seasonal variability in the tropics (Figure 2). These overall seasonal responses are also generally in agreement with the CZCS. Initial conditions of chlorophyll were homogeneous fields horizontally and vertically [*Gregg*, 2000].

Correlation analysis was executed to evaluate the agreement and departures of the seasonal distributions of chlorophyll computed by the model from the CZCS. Model basin-scale seasonal distributions of chlorophyll agree to the 95% confidence level with the CZCS in 9 out of the 12 major basins (Figure 3). The three regions that do not exhibit statistically significant positive correlation are the North Pacific, the equatorial Pacific, and the Antarctic. The equatorial Pacific exhibits almost no seasonal variability in CZCS chlorophyll as a basin mean, which is properly indicated by the model, and so this is an artifact of correlation analysis, and in reality agreement exists. There is significant bias between the results, however.

In the North Pacific, the lack of statistical correlation between the model and the CZCS is due to the large values in the autumn and winter in the CZCS, when the model predicts low values. A similar, but not as large, effect is apparent in the North Atlantic. The model-computed maximum

value in the summer North Pacific is larger than the CZCS, but the timing is matched, as is the increase from winter through early spring.

In the Antarctic, the model predicts a bloom-and-recede seasonal pattern similar to the northern sub-polar basins, while the CZCS exhibits almost no response, at least from January through August (Figure 2). This gives rise to the lack of statistical correlation here (Figure 3). However, CZCS chlorophyll concentrations from September though December indicate a build up to a spring/summer bloom, as does the model.

The North Indian Ocean exhibits statistically significant correlation between the model and CZCS, and most of the time there is agreement in the magnitudes as well. However, the CZCS August mean chlorophyll value for this region is about 6 times larger than the model. The CZCS mean chlorophyll, at 1.09 mg m^{-3}, represents the largest monthly mean value in the CZCS record.

The global annual mean difference between CZCS and the model is 48%, which is a bias as the model is always higher. Regional differences only occasionally exceed 100% by season, except for the equatorial Pacific, which averages 111% higher in the model for al 12 months.

3.2 Seasonal Trends in Chlorophyll: Basin Scale Comparisons with SeaWiFS

SeaWiFS basin-scale mean chlorophyll values exhibit the same general spatial and seasonal trends as the CZCS, and consequently also agree with the model at this level of comparison (Figure 4). There are some interesting differences in the SeaWiFS basin means as compared to the CZCS, however. First, the Antarctic clearly exhibits a seasonal trend in SeaWiFS data, with a bloom-and-recede pattern more similar to the northern sub-polar regions and the model predictions. The autumn high chlorophyll concentrations observed by the CZCS in the North Pacific and Atlantic are diminished, producing better agreement with the model results. Also, SeaWiFS chlorophyll values

in both the equatorial Indian and Pacific basins are much larger, so that now the model underestimates the Indian where it agreed with the CZCS, and the model exhibits no bias with respect to the Pacific whereas before it was biased high.

Correlation analyses shows that statistical significance is achieved between the model and SeaWiFS in every oceanographic basin at the 95% confidence level (Figure 5). An exception is the tropical Pacific but again the lack of seasonal variability in both the model and SeaWiFS obscures the agreement in the correlation analysis.

The agreement in the North Indian Ocean is poorer than the CZCS comparison (Figure 4). Although the maximum value in the SeaWiFS August mean is lower (0.74 mg m^{-3} compared to 1.09 mg m^{-3} for CZCS), the other months suggest an underestimate by the model. Also, the model appears to overestimate chlorophyll in the Antarctic at the summer bloom peak. The seasonal trend of the model in the equatorial Atlantic is more in conformance with SeaWiFS than with the CZCS, as the correlation coefficients suggest (0.61 for CZCS; 0.70 for SeaWiFS).

The global annual mean difference between SeaWiFS and the model is 3%, which does not represent a bias. The absolute mean difference is 13%. No region ever exceeds 80% difference for any season. The largest differences occur in the North Indian Ocean, which is regularly 70-80% larger in SeaWiFS than in the model.

3.3 Synoptic Scale Comparisons of Chlorophyll with CZCS, SeaWiFS, and *In situ* Data

Imagery of simulated chlorophyll provides a view of the nature and spatial distributions of the seasonal variability and how it compares to satellite and *in situ* data. Four months are chosen to represent some of the range of seasonal variability exhibited by the model and observed in SeaWiFS

and the CZCS (Figures 6 and 7). Generally, large-scale features are represented in the model and conform to CZCS and SeaWiFS data: vast areas of low chlorophyll in the mid-ocean gyres, elevated chlorophyll in the equatorial and coastal upwelling regions, and large concentrations in the sub-polar regions. The large scale features of the seasonal variability are represented as well: blooms of chlorophyll in local spring/summer in the high latitudes, followed by retreat in the local winter; expansion of low chlorophyll gyre regions in local summer, followed by contraction in winter; enhancement in the Indian Ocean in August and December, and reduced concentrations in February and May.

February represents a transition period, when phytoplankton growth in the Southern Hemisphere is diminishing and growth in the Northern Hemisphere has not yet begun (Figure 6). Relatively low chlorophyll concentrations exist north of about 50° N with bands of moderate chlorophyll at the sub-polar convergence zone. Remnants of the Southern Hemisphere bloom are still apparent in SeaWiFS imagery, especially near New Zealand, the Scotian Sea, and especially offshore of the Patagonian shelf. These features are generally represented by the model, but the spatial variability in SeaWiFS is much larger. The model shows very low chlorophyll in proximity of the ice fields in the Weddell and Ross seas, while SeaWiFS is higher.

The sub-polar transition zones in the South Atlantic, Indian, and Pacific Oceans are represented in the model, although the model exhibits generally larger concentrations and less spatial variability in the Indian and Pacific sectors. The North Central Pacific gyre is about the same size in the model as in SeaWiFS, but the Southern Hemisphere mid-ocean gyres are somewhat larger.

The tropical Pacific upwelling region has larger chlorophyll concentrations in the model than SeaWiFS, but the meridional and zonal extent is similar (Figure 6). Upwelling off the Mauritanian and Namibian coasts is represented in the model, although with reduced peak values. The model

underestimates the chlorophyll concentrations in the Arabian Sea and North Indian Ocean. High chlorophyll offshore of Costa Rica is apparent in both. The California coast exhibits strong upwelling in both the model and imagery.

In May the Northern Hemisphere spring bloom is in full swing in CZCS imagery, and is apparent in the model (Figure 7). The northerly extent of the bloom extends to the edge of the model domain in the CZCS imagery, and nearly so in the model. There is more spatial variability in the North Pacific in the CZCS than in the model, but magnitudes and extent are similar. There are many specific features of the North Atlantic bloom that differ between model and CZCS, but the overall structure and magnitude is similar.

The North Pacific and Atlantic gyres exhibit expansion from February in both the model and CZCS. The shapes of the mid-ocean gyre regions do not conform, because of slightly larger values in the model at the periphery of the gyre in the Pacific (0.08-0.1 mg m^{-3} in the model compared to 0.04-0.08 mg m^{-3} in the CZCS).

The Southern Hemisphere gyres exhibit some contraction in May compared to February (Figure 6). Sizes and magnitudes appear to be represented in the model. The Patagonian and South Atlantic sub-polar transition zones are both diminished in chlorophyll relative to February. The Australia/New Zealand region of high pigment in CZCS is reduced in magnitude and extent in May, as it also is in the model, but the model appears to underestimate the magnitude. Coverage south of -50° latitude is sparse in the CZCS, and the model is the only source of data. Where CZCS data exist, they appear to be in agreement with the model.

In August chlorophyll concentrations have fallen slightly in the model in the North Pacific and Atlantic, but appear to be sustained in the CZCS. The model now exhibits high chlorophyll to the

northern edge of the domain, as does the CZCS. Very large expansion of the Northern Hemisphere mid-ocean gyres has occurred, in both model and CZCS.

Large pigment biomasses are observed in the CZCS in the North Indian Ocean and Arabian Sea. As noted earlier, the August North Indian is the largest mean biomass observed by the CZCS in its entire history. The model also shows major increases in chlorophyll concentrations, due to the intensification of the southwest monsoon, but is not nearly as dramatic.

Enhancement of CZCS pigment in the tropical Atlantic is very strong in August, as is chlorophyll in the model (Figure 7). Large pigment concentrations are apparent in the CZCS along the Namibian coast. There is substantial contraction of the Southern Hemisphere gyres, along with some modest enhancement of the Patagonian pigment. These patterns are represented by the model. The observed portions of the Antarctic Ocean and sub-polar transition zones have larger mean pigment concentrations in the CZCS compared to May, as well as in the model. An exception is the diminished pigment near New Zealand, for which the opposite trend is found in the model. The model predicts very low biomasses south of –50° latitude. CZCS data are either obscured by clouds or unsampled, but the slivers that exist (e.g., near 180° W) suggest agreement with the model.

December SeaWiFS chlorophyll concentrations exhibit major reduction in magnitude in the North Pacific and Atlantic, along with contraction of the Northern Hemisphere mid-ocean gyres as the sub-polar regions of high pigment have moved south (Figure 7). These trends are represented by the model. There is intensification of chlorophyll biomass in SeaWiFS along the western US coast that is not represented by the model. Again the model predicts larger chlorophyll concentrations in the tropical Pacific than SeaWiFS, but the extent is similar. Note especially the area of high chlorophyll north of the main axis of the tropical upwelling located between 160°W and 100°W at the confluence of the California current and the beginning of the North Equatorial current, which is also apparent in

SeaWiFS. The tropical Atlantic shows a decrease in chlorophyll in SeaWiFS from August, as does the model. High chlorophyll off the coast of Namibia has grown in the model and SeaWiFS from August. The tropical and North Indian Ocean, and the Arabian Sea, are reduced in chlorophyll in both the model and SeaWiFS from August, but are still much larger than in May and are much larger in SeaWiFS. Southern Hemisphere gyres begin to exhibit expansion from their distribution in August, and the southern ocean is now dramatically increasing in chlorophyll. The model represents these trends, but SeaWiFS shows much greater spatial variability than the model.

A comparison of seasonal trends in model chlorophyll with the *in situ* archive shows similar features to the model/satellite comparisons (Figure 8). Overall, large-scale features are in general agreement. Substantial reduction in chlorophyll can be observed in the northern high latitudes from summer to autumn, but more so in the model than in the *in situ* data. Equatorial upwelling is present in both in the Atlantic and Pacific, and the Atlantic appears to diminish somewhat from summer to autumn. The model-computed chlorophyll in the equatorial Pacific exceeds the *in situ* data, as with the CZCS, but there is an intensification of the Peru upwelling from summer to autumn in both. As with the CZCS and SeaWiFS, the *in situ* data exhibit much larger chlorophyll concentrations in the Arabian Sea in both seasons than the model, but not generally in the North Indian Ocean. The southern ocean shows dramatic increases from summer to autumn, but the *in situ* data, like the satellite data, indicate much more spatial variability than the model.

3.4 Seasonal Trends in Nitrate: Synoptic Scale Comparisons with *In situ* Data

Model surface nitrate results are averaged over seasons and compared to *in situ* archives maintained by NODC/OCL [*Conkright et al.*, 1998b; 1998c; 1998d]. The results show overall agreement between model and data, and features of seasonal variability are in conformance (Figures

9 and 10). Spatial distributions and magnitudes are represented by the model. Year-to-year nitrate differences in the model are < 0.5% by the beginning of the third year of simulation, suggesting that deep nitrate concentrations have equilibrated and the results shown here are not driven by the initial conditions. A seven-year run confirmed this observation. Two general exceptions to the overall agreement are the tropical Pacific and Atlantic. In both cases the model predicts much larger nitrate concentrations than are observed in the data. The departure is much reduced for summer and autumn in the Pacific, but the discrepancy in the Atlantic is persistent and large. *In situ* data show little apparent evidence of upwelling in the Atlantic, whereas the model exhibits strong upwelling.

Note how seasonal distributions of nitrate are represented in the North Pacific and Atlantic by the *in situ* data and the correspondence in model results (Figures 9 and 10). Large concentrations, with magnitudes and spatial extent matching the data, are apparent in winter, which diminish in spring. By summer magnitudes reach a minimum, and begin to recover by autumn. The reduction of nitrate is much greater in the North Atlantic than in the Pacific. The Arabian Sea exhibits moderate nitrate values in winter, diminishing in spring, and attaining the maximum in summer.

4. Discussion

A comparison of computed chlorophyll and nutrients from a coupled general circulation, biogeochemical, radiative model of the global oceans with satellite and *in situ* data sources produces many encouraging results. Generally, large-scale chlorophyll features such as the location, size, and shape of mid-ocean gyres, equatorial upwelling regions, high latitudes, and coastal upwelling regions are in broad agreement with CZCS and SeaWiFS chlorophyll values. Basin-scale (>1000 km) seasonal distributions of chlorophyll are statistically positively correlated with CZCS in 10 out of 12

major oceanographic regions, and with SeaWiFS in all regions. Global annual mean chlorophyll values agree with CZCS to within 48% and with SeaWiFS to within 13%.

On synoptic scales (100-1000 km), results are not as positive, but contain some encouraging aspects. The mid-ocean gyres expand in the local summer and contract in local winter, simulating cycles indicated in the CZCS and SeaWiFS. In the model these trends are the result of mixed layer deepening in local winter, injecting nutrients into the previously exhausted mixed layer, and stimulating modest phytoplankton growth. The growth remains modest because the mixed layer depths are still relatively large producing an overall low irradiance level that prevents explosive growth. At the high latitudes, rapid mixed layer shoaling resulting from heating and reduced wind stresses provides a high light environment, coupled with reduced solar zenith angles and long daylengths, that produces large phytoplankton growth and large chlorophyll concentrations characteristic of the spring/summer bloom at these locations. The tropics exhibit reduced seasonality in general, which is represented by the model. Global synoptic scale patterns of nitrate seasonal dynamics are in agreement with NODC/OCL climatological seasonal data.

The advantage of numerical simulation modeling is that processes governing model results are completely understood. When model results agree with data, it suggests that the processes in the model causing the similar result are valid, and we can gain a fundamental understanding of the data. Such agreement occurs in this analysis of the seasonal variability of the global oceans in many aspects of the basin-scale and synoptic scale results as compared to satellite and *in situ* data. However, an understated aspect of numerical modeling is that when the results do not agree with available data, then it indicates the importance of excluded processes.

In this analysis of the results of a coupled general ocean physical/biogeochemical/radiative model, there are four main areas of disagreement between the model and available data sets. These are 1)

overestimation of model chlorophyll in the spring/summer maximum in southern ocean, along with inadequate spatial variability, 2) overestimation of model chlorophyll in the tropical Pacific, 3) inability of the model to represent late summer/autumn chlorophyll concentrations in the northern high latitudes, and 4) underestimation of the model of the seasonal dynamics in the North Indian Ocean.

All three evaluation data sets indicated that the Antarctic basin has large spatial variability, with local maxima located near Australia and New Zealand, offshore of Patagonia and South Africa, and across the South Atlantic sub-polar convergence zone. Although the model also exhibits these features, it also predicts large chlorophyll biomasses across the eastern South Pacific sub-polar convergence zone that the data sets do not. The CZCS does not exhibit seasonal variability, but both SeaWiFS and the *in situ* data archive do. This is probably due to poor sampling by the CZCS. Although the length of the CZCS record makes it a better representation of chlorophyll climatology, its limited and poorly distributed sampling can produce poor results at times, such as the Southern Hemisphere in particular.

The Antarctic region is a bloom-recede region similar to the northern Pacific and Atlantic, governed by the solar cycle and its influences on mixed layer depth and irradiance availability. Massive amounts of nutrients become available through upwelling and turbulent mixing in the local winter (Figure 9). With the availability of light and nutrients, the region is capable of producing a substantial spring/summer bloom, as indicated by the model. Deep mixed layers in this region inhibit a bloom of the magnitude of those observed in the North Pacific and Atlantic. Austral summer mixed layers here are the deepest in the global oceans, averaging about 50-70 m. The nutrients are also widely distributed in this region, leading to the lack of spatial variability observed in the model chlorophyll.

The Antarctic, along with the eastern tropical Pacific, is known as a high nutrient-low chlorophyll region [*Cullen*, 1991], because data sets indicate lower chlorophyll concentrations than would be expected from the available nutrients. This has given rise to the concept that phytoplankton populations are limited by iron [*Martin et al.*, 1990], which has been confirmed in small-scale experiments. Iron limitation could explain some of the spatial variability in the Antarctic: Australia and New Zealand represent a potential iron-containing aerosol source, as do the Argentina plains. Other contributing influences to the lack of correspondence between model and satellite data may be the lack of circulation or mixing variability that is unavailable in the reduced gravity representation of the circulation model or the importance of eddy scale processes [*McGillicuddy et al.*, 1998; *Oschlies and Garcon*, 1998].

The model also shows very low chlorophyll in proximity of the ice distribution, while the data sets indicate somewhat higher values, although variable. Low chlorophyll concentrations near the ice sheets in the model are due to very cold temperatures, limiting the maximum growth rate. Coupled with continued sinking throughout the austral winter, phytoplankton populations become too small to sustain themselves for the duration of the non-growth season. This is in spite of reduced grazing accompanying the low temperatures [*Gregg*, 2000]. The model requires a formulation of ice algal dynamics, and austral spring melting and seeding in order to reasonably simulate this area. Such dynamics have been shown to be substantial contributors to the total primary production in these regions [*Arrigo et al.*, 1997].

The tropical Pacific upwelling region has about twice the chlorophyll concentration in the model as in CZCS chlorophyll, but the meridional and zonal extent is nearly the same (Figure 2). The model agrees with SeaWiFS chlorophyll, but the SeaWiFS observations here were dominated by a record El-niño event from launch until May 1998, and then a strong La-niña event until at least February

2000, and is probably not representative of a climatology. There are indications that the model does not overestimate chlorophyll as much as the CZCS indicates. *In situ* chlorophyll data suggest mean concentrations between 0.1 and 0.2 mg m^{-3} [*Conkright et al.*, 1998c], which is more in agreement with the model means (about 0.17 mg m^{-3}), and in contrast to the CZCS (which has a mean of about 0.07-0.08 mg m^{-3}). A blended data set composed of *in situ* data and CZCS data indicated that CZCS chlorophyll estimates are about 25-40% too low in the tropical Pacific [*Gregg and Conkright*, 2000]. Nevertheless, model chlorophyll appears to overestimate the data sets. A similar result was found by *Chai et al.* [1996]. These results suggest either excessive upwelling in the model or the lack of iron as a limiting nutrient in the model. Like the Antarctic, the eastern equatorial Pacific is widely regarded as iron-limited [*Kolber et al.*, 1994; *Coale et al.*, 1998].

The model conforms to satellite and *in situ* data in predicting a distinct and large spring/summer bloom in the North Pacific and Atlantic Basins (Figures 2, 4, and 6). However, in both regions the data sets indicate that the elevated chlorophyll biomass extends well into autumn, while the model predicts a rather sharp die-off, especially in the North Pacific. The CZCS shows a boreal autumn bloom in the North Pacific (Figure 2). In the model, these regions are characterized by large changes in surface mixed layer depth, and a large variability in irradiance, due to the seasonal variability in solar zenith angle and day length. This gives rise to mixed layer deepening in winter that, coupled with low irradiance, prevents significant phytoplankton growth. Turbulence and convective overturn provide nutrients to the surface layer that cannot be utilized. Upon the arrival of spring/summer, solar irradiance increases and increased surface heating leads to shallower mixed layer depths. This provides the conditions for an extensive spring/summer phytoplankton bloom.

The late fall bloom in the CZCS, occurring in October-November, could be the result of mixed layer deepening and injection of nutrients. Similar discrepancies between model and satellite data

were observed by *Dutkiewicz et al.* [2000], *Sarmiento et al.* [1993], and *Fasham et al.* [1993] in the North Atlantic. *Sarmiento et al.* [1993] attributed the disparity to poor quality CZCS data. *Yoder et al.* [1993] asserted that CZCS data were unreliable north of 40° N in the autumn and winter months. The autumn bloom is not as prominent in SeaWiFS data, which supports *Yoder et al.* [1993], since it is a superior sensor with vastly reduced sampling bias. However, there is still an indication of a minor autumn bloom in SeaWiFS data in the North Pacific, and the receding of the summer peak in the North Atlantic is still slower than the model (Figure 4). Furthermore, *in situ* data generally support SeaWiFS data.

There are a number of possible explanations for the rapidly diminishing chlorophyll concentrations in the model that are not apparent in the data sets. Death/ingestion/sinking losses could be overestimated in the model. Phytoplankton species replacement to an even more slowly sinking group than chlorophytes could occur (see *Gregg* [2000]). Mixed layer deepening in the model may be too slow to bring nutrients to the euphotic zone soon enough before irradiance levels fall. Cloud liquid water path data could be overestimated in the International Satellite Cloud Climatology Project data sets used to drive surface irradiance. Diurnal variability in mixed layer depths or eddy-induced upwelling could bring nutrients into the euphotic zone.

The seasonal variability of the North Indian in the model also appears to be in agreement with the CZCS and SeaWiFS (Figures 2-5), with maxima corresponding to the southwest monsoon in August and the less vigorous northeast monsoon in winter. However, the model appears to vastly underestimate the magnitude of the southwest monsoon observed by the CZCS at the peak in August. The disparity between the model and SeaWiFS in August is not quite as large (Figure 4). Large chlorophyll concentrations are expected here this time of year, since it corresponds to the peak of the southwest monsoon. Winds during this time of year can exceed 12 m s^{-1} as a monthly mean,

which drives vigorous mixing, nutrient availability, and associated phytoplankton growth. Associated with the strong winds is thick cloud cover (exceeding 80% as a monthly mean, with cloud optical thickness of 4 or more), which in the model tends to suppress vigorous growth. *In situ* records during the southwest monsoon [*Conkright et al.*, 1998d] range from about 0.3 to 0.7 mg m^{-3} in the Arabian Sea (Figure 8). This is less than the CZCS and SeaWiFS but still greater than the model range of about 0.15 to 0.45 mg m^{-3}. *Gardner et al.* [1999] reported maximum surface values of about 3 mg m^{-3} during the late southwest monsoon, which quickly dissipated to about 1.2 mg m^{-3} in two days. The CZCS observes >3 mg m^{-3} over large parts of the Arabian Sea, which may be suspect because of the presence of absorbing aerosols originating from nearby desert regions. These absorbing aerosols are incorrectly identified in the CZCS processing, and result in overestimates of chlorophyll if they are present because they absorb blue radiance like chlorophyll. SeaWiFS monthly means are reduced because the aerosols are so thick that they fail aerosol optical thickness tests in the algorithms, and thus do not contribute to the basin mean.

On the other hand, agreement of the model with SeaWiFS data during the northeast monsoon is poorer than with the CZCS (Figures 2 and 4). This is because the aerosol characterization by CZCS is less inaccurate for these aerosols than SeaWiFS, which is usually a considerably superior sensor. Thus for SeaWiFS, not only do the dust aerosols resemble chlorophyll, but mischaracterization of their spectral nature by the SeaWiFS atmospheric correction algorithms exacerbates the problem. Despite these problems with satellite observations of the North Indian ocean and Arabian Sea, the model appears incapable of capturing the dramatic responses of phytoplankton to the monsoons here, as compared to *in situ* data. These problems are most likely related to the circulation model, with lack of bottom topographic effects and possibly also the absence of coastal influences. Deficiencies in circulation models are a common problem for biogeochemical analyses [*Doney*, 1999]

Although model surface nitrate results show overall agreement between model and data (Figures 9 and 10), two general exceptions are the tropical Pacific and Atlantic. In both cases the model predicts much larger nitrate concentrations than are observed in the data. The departure is much reduced for summer and autumn in the Pacific, but the discrepancy in the Atlantic is persistent and large. *In situ* data show little apparent evidence of upwelling in the Atlantic, whereas the model exhibits strong upwelling. The satellite and *in situ* data clearly show high chlorophyll biomasses indicative of upwelling (Figures 6-8). The conditions present, e.g., winds, coastal boundary, equatorial divergence, suggest upwelling, which is not supported by the *in situ* nitrate data. Large nitrate concentrations exist at 50-100 m in the *in situ* archive, suggesting immediate uptake by the phytoplankton as it advects/diffuses across the mixed layer.

Despite these and other problems, there are many examples of overall broad agreement of the model results with satellite and *in situ* data. These areas of agreement are attributed to the generalized, process-oriented approach and the existence of multiple phytoplankton groups with different physical, physiological, and optical properties [*Gregg*, 2000]. Included processes such as viscosity-dependent sinking rates, temperature-dependent phytoplankton growth and herbivore grazing responses, photoadaptation and carbon:chlorophyll states based on irradiance in the water column, and nitrogen fixation [*Gregg*, 2000] are pivotal for enabling biogeochemical constituents to adapt to the diversity of global environments without regional parameterization. These represent fundamental physical and biogeochemical processes, many of which are considered necessary for improvement of biogeochemical models [*Doney*, 1999]. While these processes are clearly insufficient at times and places in the global model, this approach provides a preliminary step toward improved understanding of the fundamental underpinnings of phytoplankton distributions.

5. Summary and Conclusions

Global computed chlorophyll and nitrate distributions from a coupled ocean general circulation, biogeochemical, and radiative model compare with satellite and *in situ* sources. Generally, large-scale chlorophyll features such as the location, size, and shape of mid-ocean gyres, equatorial upwelling regions, high latitudes, and coastal upwelling regions are in broad agreement with CZCS, SeaWiFS, and *in situ* data sources. Basin-scale seasonal dynamics from the model are significantly positively correlated with CZCS data in 10 of 12 major oceanographic regions, and with SeaWiFS in all 12. Shifts of high chlorophyll across hemispheres are in correspondence, as are timing features of bloom-and-recede. The mid-ocean gyres expand in the local summer and contract in local winter in accordance with mixed layer shallowing and deepening, respectively, and resemble cycles indicated in the CZCS and SeaWiFS.

Seasonal comparisons with *in situ* nitrate climatologies also exhibit correspondence. The location, seasonal dynamics, and magnitudes are apparent in the model. A notable exception is the equatorial Atlantic upwelling region, which appears prominently in the model but is not indicated in the data.

There are several significant discrepancies between model results and data. For example, the tropical Pacific appears overestimated in the model. Spatial variability in the sub-polar Southern Hemisphere is not represented well by the model. The northern high latitude basins exhibit sustained chlorophyll concentrations well into late autumn and are not predicted by the model. There are processes that may be important that are not included in the model, such as iron limitation, eddy scale processes, and topographic influences on circulation. But these discrepancies do not appear to adversely affect the overall agreement of the model with observations at synoptic and basin scales.

Considering that the model is initialized with flat fields of chlorophyll, this suggests a degree of realism in the physical, biological, and radiative dynamics included in the model, at least at basin and synoptic scales. These results provide encouragement that more complete and comprehensive models of the global oceans than this preliminary effort can represent the diversity of global biogeochemical processes.

Acknowledgements. This paper was not possible without the development of the Poseidon GCM by Paul Schopf, George Mason University Center for Ocean-Land-Atmospheres, and the provision of code for integration. Michele Rienecker, NASA/GSFC, provided meaningful insight into the GCM results and dynamics. The NASA/Goddard Space Flight Center Distributed Active Archive Center provided the CZCS data that was used for comparison. Margarita E. Conkright (NODC/OCL) provided *in situ* nitrate and chlorophyll seasonal climatologies. This work was supported under NASA Grant (RTOP) 971-622-51-31.

References

Arrigo, K.R., D.L. Worthen, M.P. Lizotte, P. Dixon, and G. Dieckmann, Primary production in Antarctic sea ice, *Science*, 276, 394-397, 1997.

Chai, F., S.T. Lindley, and R.T. Barber, Origin and maintenance of a high nitrate condition in the equatorial Pacific, *Deep-Sea Res.*, 43, 1031-1064, 1996.

Coale, K.H., K.S. Johnson, S.E. Fitzwater, S.O.G. Blain, T.P. Stanton, and T.L. Coley, Iron Ex-I, and *in situ* iron-enrichment experiment: Experimental design, implementation, and results, *Deep-Sea Res.*, 45, 919-945, 1998.

Conkright, M.E. and W.W. Gregg, Comparison of chlorophyll climatologies: *in situ*, CZCS, blended *in situ*-CZCS, and SeaWiFS. *Global Biogeochem. Cycles*, submitted, 2000.

Conkright, M.E., S. Levitus, T.O'Brien, T.P. Boyer, C. Stephens, D. Johnson, L. Stathoplos, O. Baranova, J. Antonov, R. Gelfeld, J. Burney, J. Rochester, and C. Forgy, World Ocean Database 1998 CD-ROM Data Set Documentation, *National Oceanographic Data Center*, Silver Spring, MD, 1998a.

Conkright, M.E., T.O'Brien, S. Levitus, T.P. Boyer, C. Stephens, J. Antonov, World ocean atlas 1998 Volume 10. Nutrients and chlorophyll of the Atlantic Ocean, *NOAA Atlas NESDIS 36*, 217pp., 1998b.

Conkright, M.E., T.O'Brien, S. Levitus, T.P. Boyer, C. Stephens, J. Antonov, World ocean atlas 1998 Volume 11. Nutrients and chlorophyll of the Pacific Ocean. *NOAA Atlas NESDIS 37*, 217pp., 1998c.

Conkright, M.E., T.O'Brien, S. Levitus, T.P. Boyer, C. Stephens, J. Antonov, World ocean atlas 1998 Volume 12. Nutrients and chlorophyll of the Indian Ocean. *NOAA Atlas NESDIS 38*, 217pp., 1998d.

Conkright, M.E., S. Levitus and T.P. Boyer, Quality Control of Historical Nutrient Data., *NOAA Technical Memorandum 79*, 75 pp., 1994.

Cullen, J.J., Hypotheses to explain high-nutrient conditions in the open sea, *Limnol. Oceanogr.* 36, 1578-1599, 1991.

Doney, S.C., Major challenges confronting marine biogeochemical modeling, *Global Biogeochem. Cycles*, 13, 705-714, 1999.

Dutkiewicz, S., M. Follows, J. Marshall, and W.W. Gregg, Interannual variability of phytoplankton abundances in the North Atlantic. *Deep-Sea Research*, in press, 2000.

Fasham, M.J.R., J.L. Sarmiento, R.D. Slater, H.W. Ducklow, and R. Williams, A seasonal three-dimensional ecosystem model of nitrogen cycling in the North Atlantic euphotic zone: A comparison of the model results with observations from Bermuda Station "S" and OWS "India", *Global Biogeochem. Cycles*, 7, 379-415, 1993.

Frouin, R., M. Schwindling, and P.-Y. Deschamps, Spectral reflectance of sea foam in the visible and near-infrared: *In situ* measurements and remote sensing implications, *J. Geophys. Res.* 101, 14361-14371, 1996.

Gardner, W.D., J.S. Gundersen, M.J. Richardson, and I.D. Walsh. The role of seasonal and diel changes in mixed-layer depth on carbon and chlorophyll distributions in the Arabian Sea. *Deep-Sea Res.* 46: 1833-1858, 1999.

Gordon, H.R. and M. Wang, Retrieval of water-leaving radiance and optical thickness over the oceans with SeaWiFS: A preliminary algorithm, *Applied Optics*, 33, 443-452, 1994.

Gregg, W.W., Seasonal Distributions of Global Ocean Chlorophyll and Nutrients with a Coupled Ocean General Circulation, Biogeochemical, and Radiative Model. I. Model Description and Phytoplankton Distributions, *J. Geophys. Res.*, submitted, 2000.

Gregg, W.W. and M.E. Conkright, Global seasonal climatologies of ocean chlorophyll: Blending in situ and satellite data for the CZCS era, *J. Geophys. Res.*, accepted for publication, 2000.

Kolber, Z.S., R.T. Barber, K.H. Coale, S.E. Fitzwater, R.M. Greene, K.S. Johnson, S. Lindley, and P.G. Falkowski, Iron limitation of phytoplankton photosynthesis in the equatorial Pacific Ocean, *Nature*, 371, 145-148, 1994.

Martin, J.H., R.M. Gordon, and S.E. Fitzwater, Iron in Antarctic waters, *Nature*, 345, 156-158, 1990.

McGillicuddy, D.J., A.R. Robinson, D.A. Siegel, H.W. Jannasch, R. Johnson, T.D. Dickey, J.

McNeil, A.F. Michaels, and A.H. Knap, Influence of mesoscale eddies on new production in the Sargasso Sea, *Nature*, 394, 263-266, 1998.

O'Reilly, J.E., S. Maritorena, B.G. Mitchell, D.A. Siegel, K.L. Carder, S.A. Garver, M. Kahru, and C. McClain, Ocean color chlorophyll algorithms for SeaWiFS. *J. Geophys. Res.*, 103, 24937-24953, 1998.

Oschlies, A. and V. Garcon, Eddy-induced enhancement of primary production in a model of the North Atlantic Ocean, *Nature*, 394, 266-269, 1998.

Sarmiento, J.L., R.D. Slater, M.J.R. Fasham, H.W. Ducklow, J.R. Toggweiler, and G.T. Evans, A seasonal three-dimensional ecosystem model of nitrogen cycling in the North Atlantic euphotic zone. *Glob. Biogeochem. Cycles*, 7, 417-450, 1993

Siegel, D.A., M. Wang, S. Maritorena, and W. Robinson, Atmospheric correction of satellite ocean color imagery: The black pixel assumption, *Appl. Opt.*, submitted, 2000.

Yoder, J.A., C.R. McClain, G.C. Feldman, and W.E. Esaias, Annual cycles of phytoplankton chlorophyll concentrations in the global ocean: a satellite view. *Global Biogeochem. Cycles*, 7, 181-193, 1993.

W.W. Gregg, NASA/Goddard Space Flight Center, Laboratory for Hydrospheric Processes, Code 971, Greenbelt, MD 20771 gregg@cabin.gsfc.nasa.gov

Figure Captions

Figure 1. Comparison of re-analyzed SeaWiFS global data with other global data sets. IS indicates the *in situ* archive maintained by NOAA/NODC, CZ indicates the CZCS, BL indicates a blended data set [*Gregg and Conkright*, 2000], SW indicates SeaWiFS data, and OC3 indicates the re-analyzed data using an NIR reflectance correction and the OC3 bio-optical algorithm. Top: Global means. Bottom: global variances. Figure is reprinted courtesy of M. Conkright, NOAA/NODC.

Figure 2. Comparison of model-generated mean chlorophyll (solid line) with climatological monthly mean CZCS chlorophyll (open squares) for the 12 major oceanographic basins in the global oceans. Error bars on the CZCS chlorophyll represent one-half the CZCS standard deviation.

Figure 3. Correlation of basin-scale mean chlorophyll values with the CZCS. The solid line indicates the best-fit, and the correlation coefficient is indicated. An asterisk indicates that the correlation is significantly positively correlated at the 95% confidence level. The probability value to establish statistical significance is 0.576. The equatorial Pacific does not indicate positive correlation because of the lack of seasonal variability in either result. However, this lack of seasonal variability in both the model and CZCS indicates agreement.

Figure 4. Comparison of model-generated mean chlorophyll (solid line) with climatological monthly mean SeaWiFS chlorophyll (open diamonds) for the 12 major oceanographic basins in the global oceans. Error bars on the SeaWiFS chlorophyll represent one-half the SeaWiFS standard deviation.

Figure 5. Correlation of basin-scale mean chlorophyll values with the SeaWiFS. The solid line indicates the best-fit, and the correlation coefficient is indicated. An asterisk indicates that the correlation is significantly positively correlated at the 95% confidence level. The probability value to establish statistical significance is 0.576. The equatorial Pacific does not indicate positive

correlation because of the lack of seasonal variability in either result. However, this lack of seasonal variability in both the model and SeaWiFS indicates agreement.

Figure 6. Model and SeaWiFS monthly mean chlorophyll distributions for February (top), and model and CZCS mean monthly pigment for May (bottom). Climatological monthly ice distributions are indicated, but are not part of the model computations.

Figure 7. Model chlorophyll and CZCS monthly mean pigment distributions for August (top), and model and SeaWiFS mean monthly chlorophyll for December (bottom). Climatological monthly ice distributions are indicated, but are not part of the model computations.

Figure 8. Seasonal distributions of model chlorophyll for summer (top) and autumn (bottom, compared to objectively analyzed fields from the NODC/OCL *in situ* archive.

Figure 9. Comparison of model-computed surface nitrate distributions (averaged over seasons) with *in situ* data archives from NODC/OCL for winter and spring. Units are μM. Model year-to-year changes were $< 0.5\%$ in the global surface layer by the third year of simulation.

Figure 10. Comparison of model-computed surface nitrate distributions (averaged over seasons) with *in situ* data archives from NODC/OCL for summer and autumn. Units are μM.

Global Chlorophyll Means

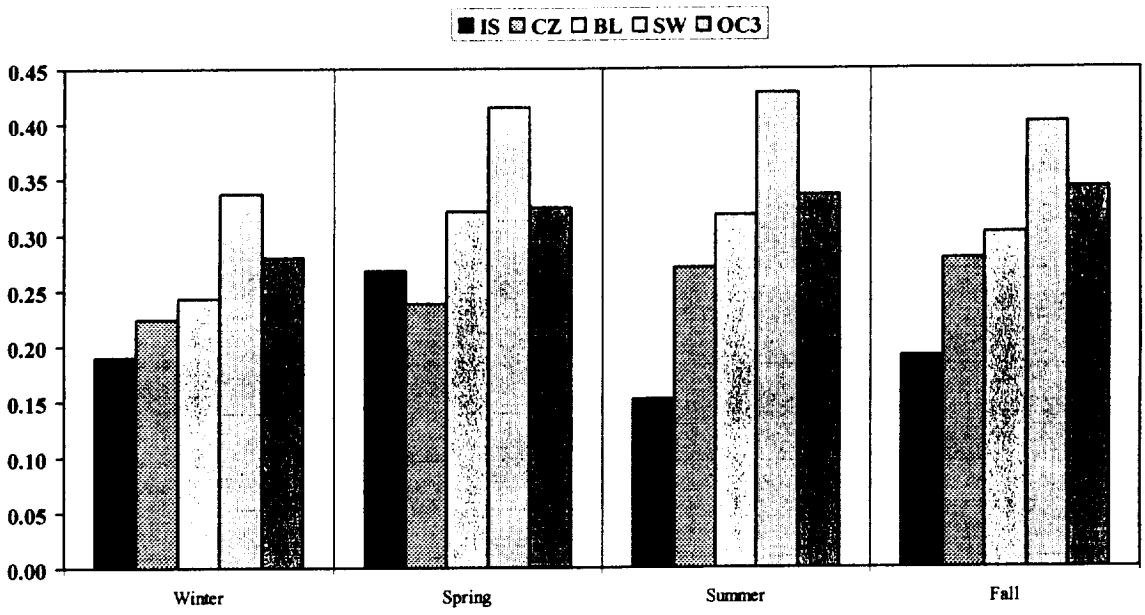

Global Chlorophyll Variances

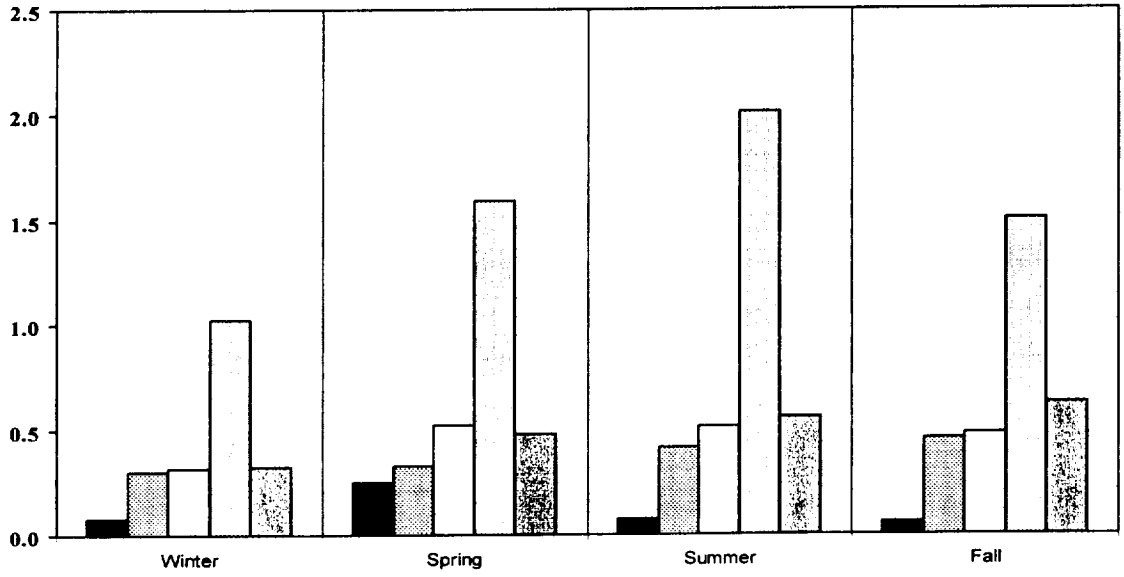

F

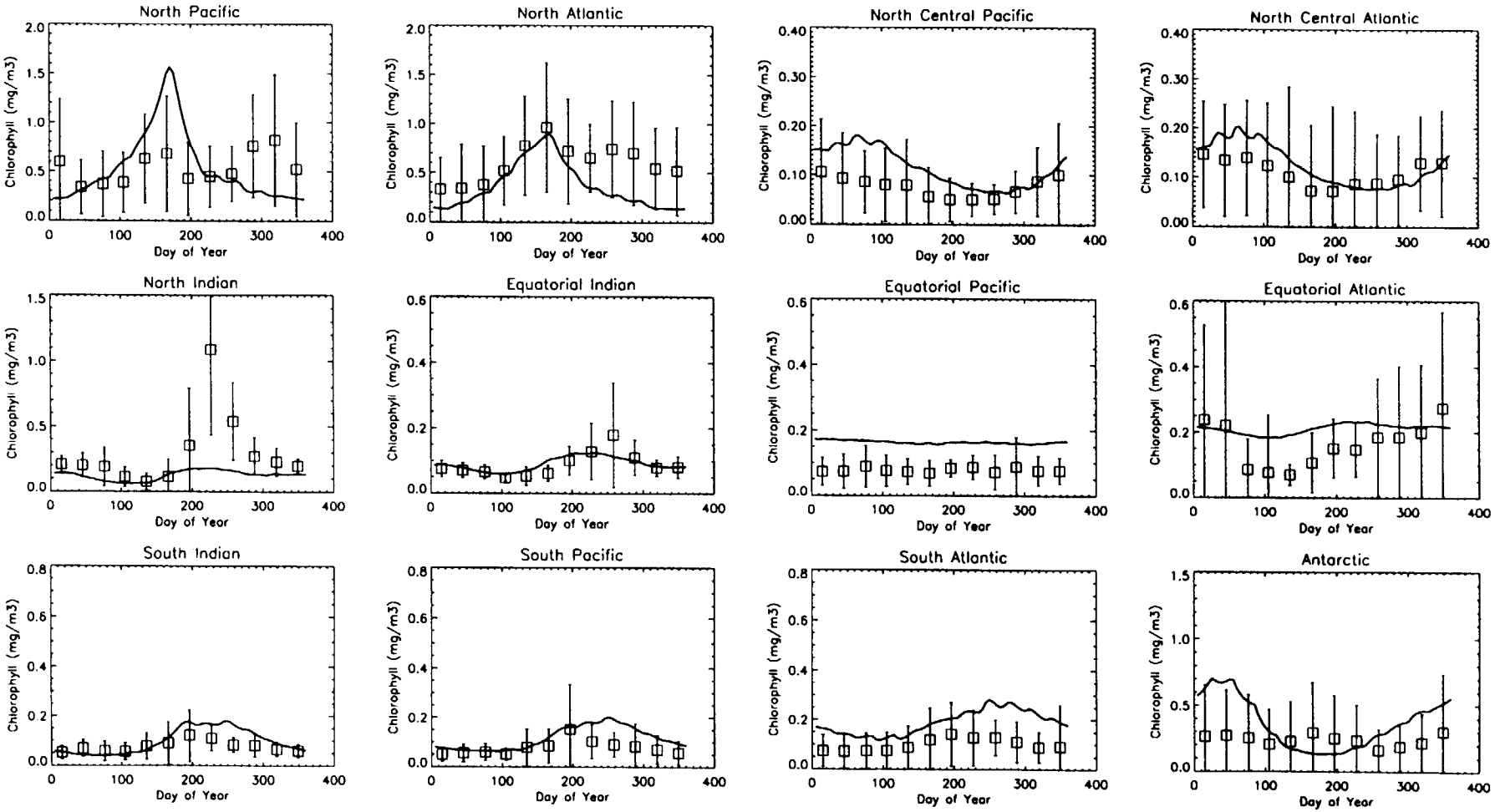
North Pacific
North Atlantic
North Central Pacific
North Central Atlantic
North Indian
Equatorial Indian
Equatorial Pacific
Equatorial Atlantic
South Indian
South Pacific
South Atlantic
Antarctic
Chlorophyll (mg/m3)
Day of Year

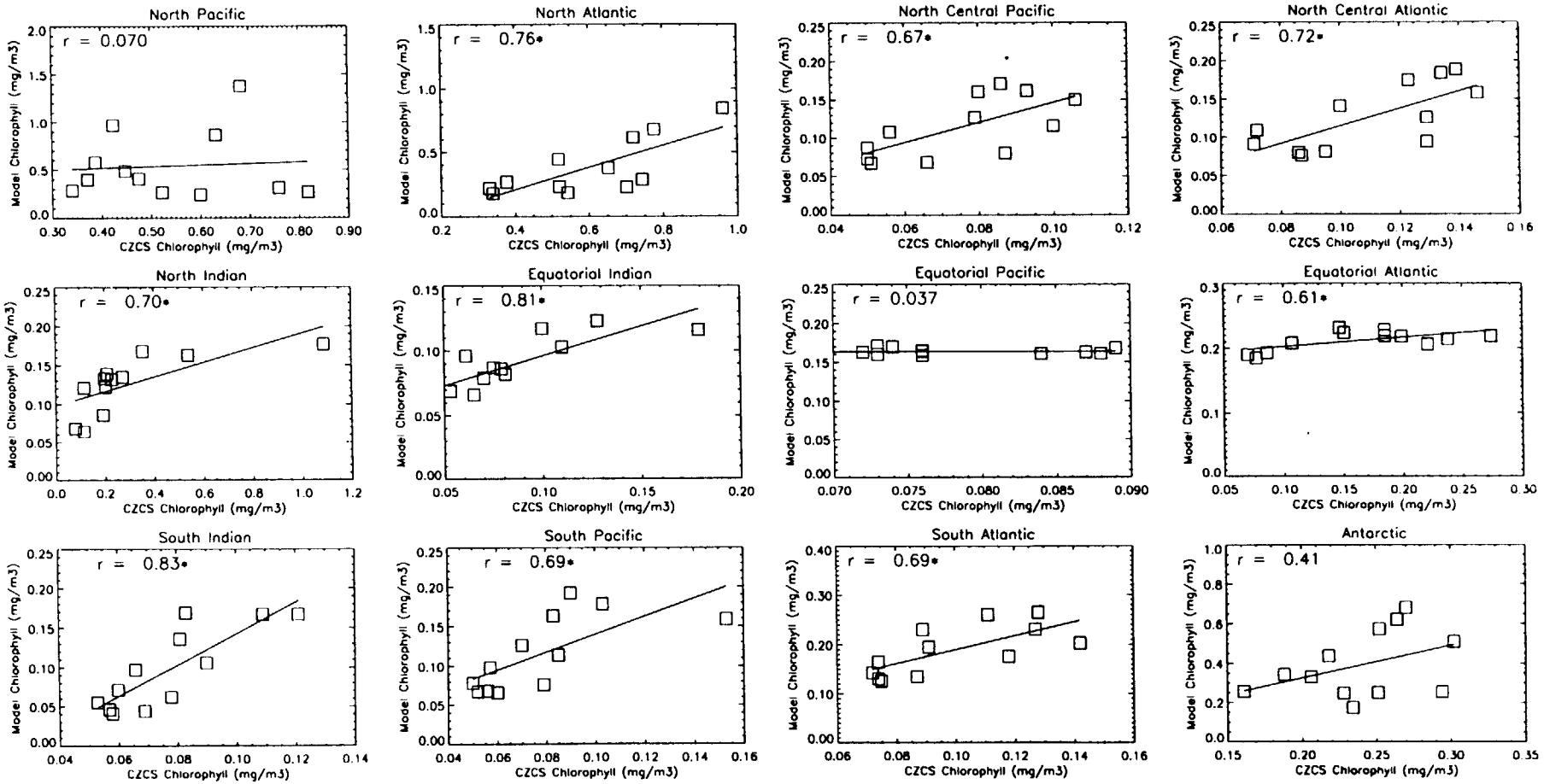
North Pacific
r = 0.070
North Atlantic
r = 0.76*
North Central Pacific
r = 0.67*
North Central Atlantic
r = 0.72*
North Indian
r = 0.70*
Equatorial Indian
r = 0.81*
Equatorial Pacific
r = 0.037
Equatorial Atlantic
r = 0.61*
South Indian
r = 0.83*
South Pacific
r = 0.69*
South Atlantic
r = 0.69*
Antarctic
r = 0.41
Model Chlorophyll (mg/m3)
CZCS Chlorophyll (mg/m3)

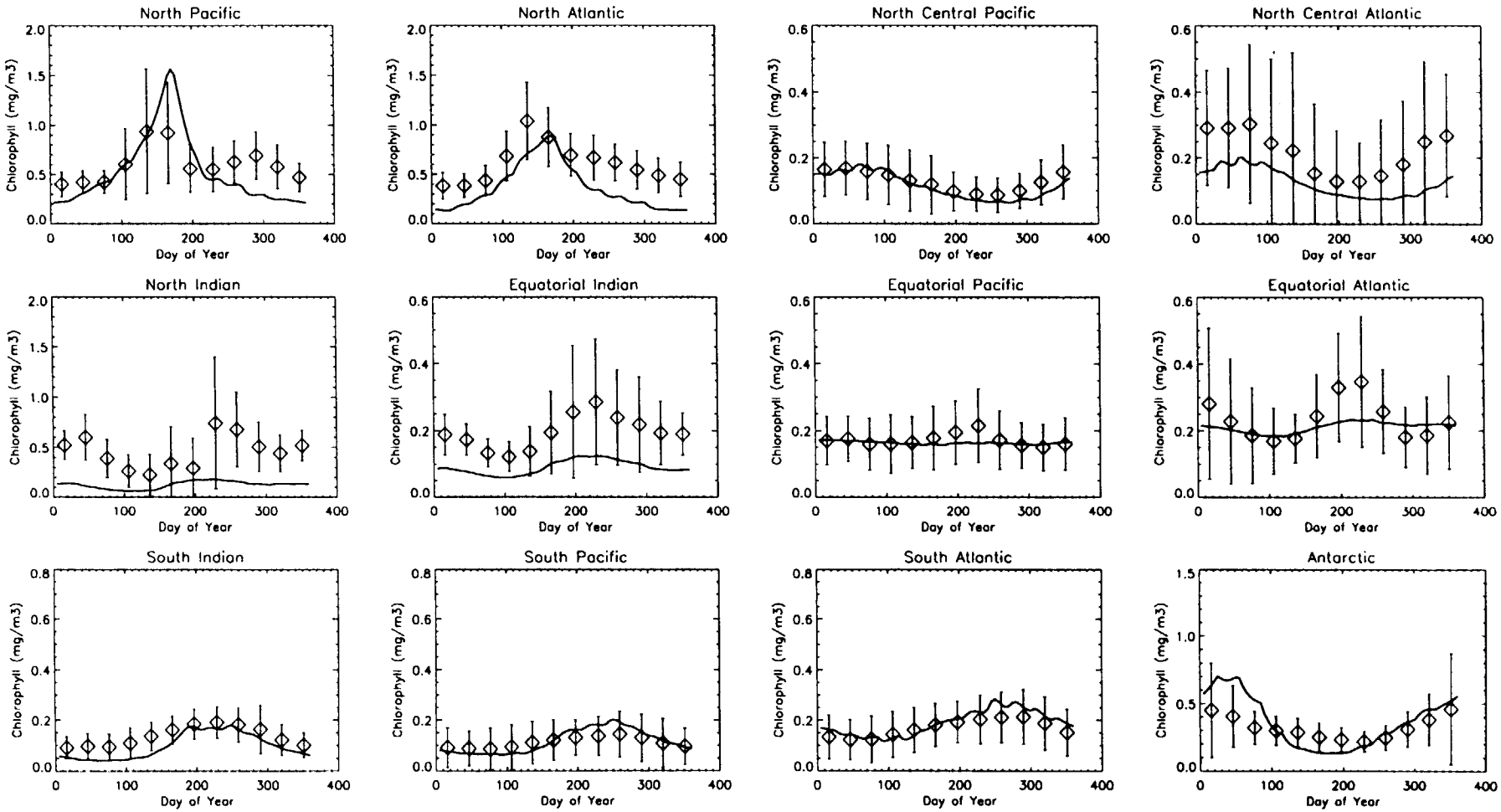
North Pacific
North Atlantic
North Central Pacific
North Central Atlantic
North Indian
Equatorial Indian
Equatorial Pacific
Equatorial Atlantic
South Indian
South Pacific
South Atlantic
Antarctic
Chlorophyll (mg/m3)
Day of Year

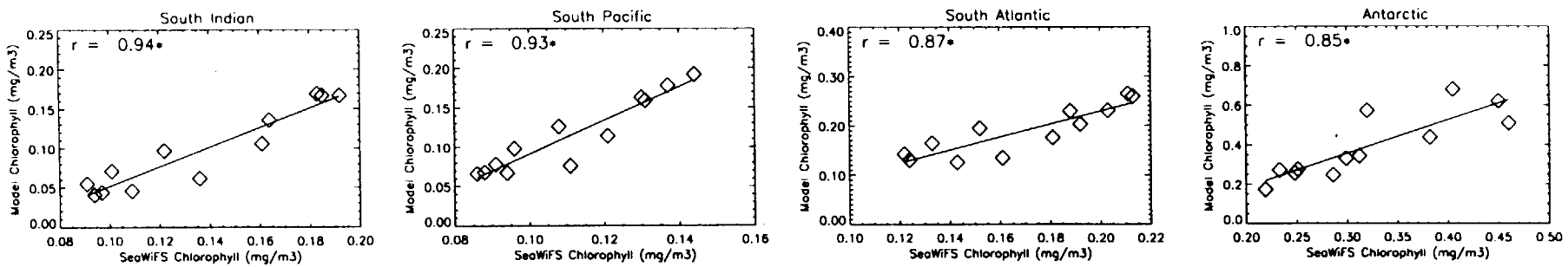
South Indian
r = 0.94*
Model Chlorophyll (mg/m3)
SeaWiFS Chlorophyll (mg/m3)
South Pacific
r = 0.93*
Model Chlorophyll (mg/m3)
SeaWiFS Chlorophyll (mg/m3)
South Atlantic
r = 0.87*
Model Chlorophyll (mg/m3)
SeaWiFS Chlorophyll (mg/m3)
Antarctic
r = 0.85*
Model Chlorophyll (mg/m3)
SeaWiFS Chlorophyll (mg/m3)

Model Chlorophyll ; February

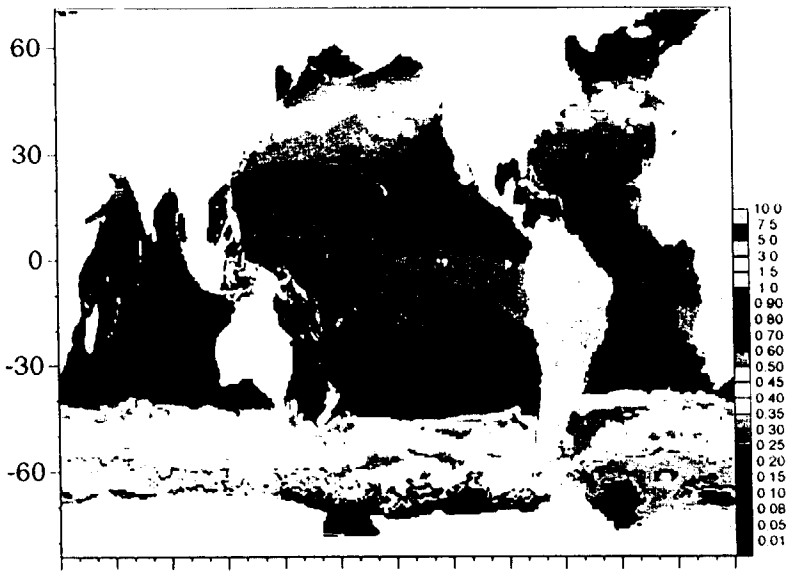

SeaWiFS Chlorophyll; February

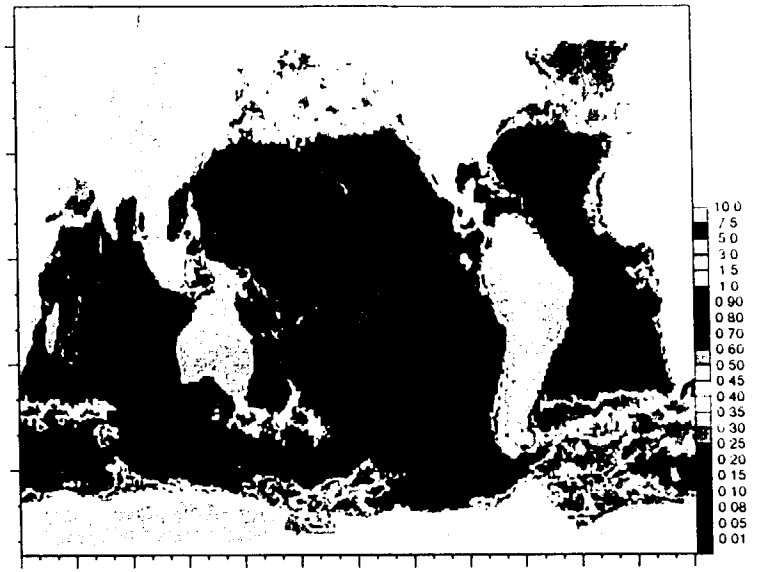

Model Chlorophyll ; May

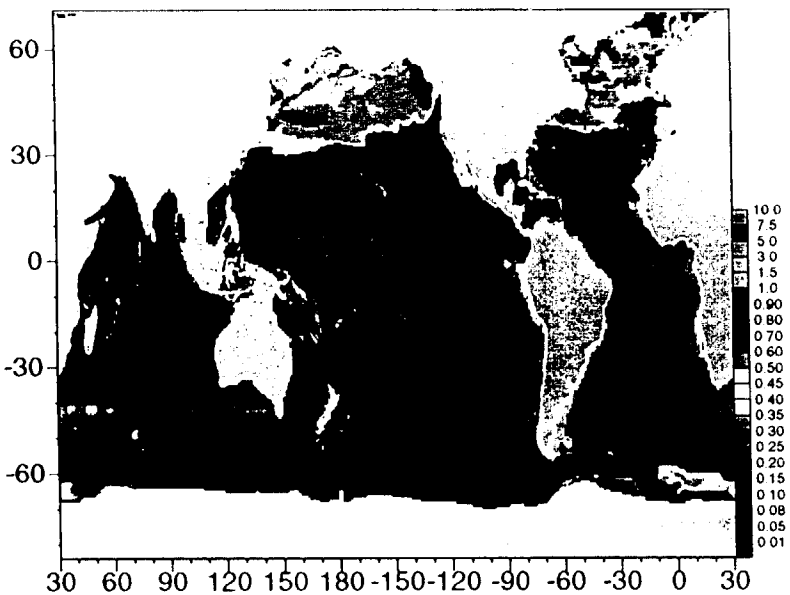

CZCS Pigment; May

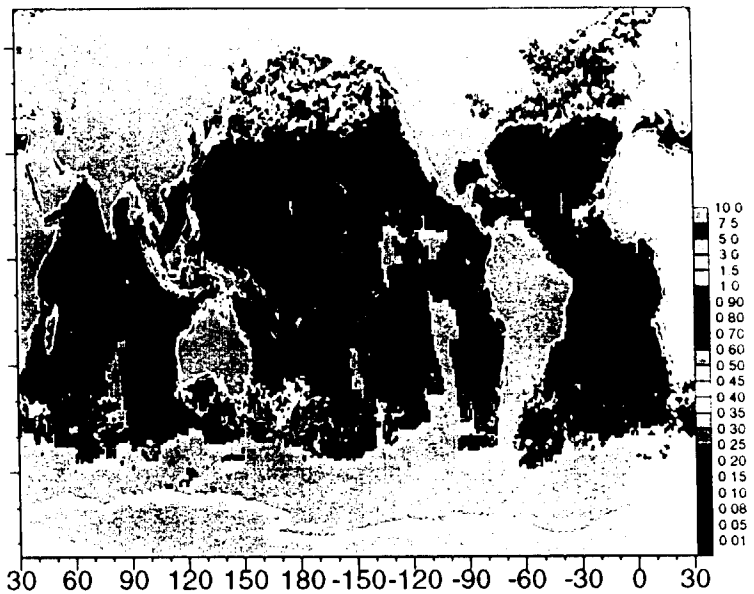

Model Chlorophyll ; August

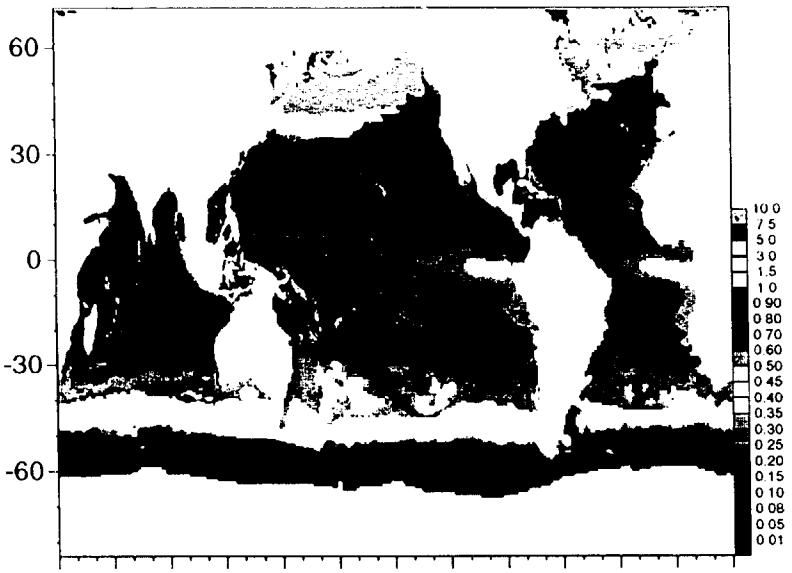

CZCS Pigment; August

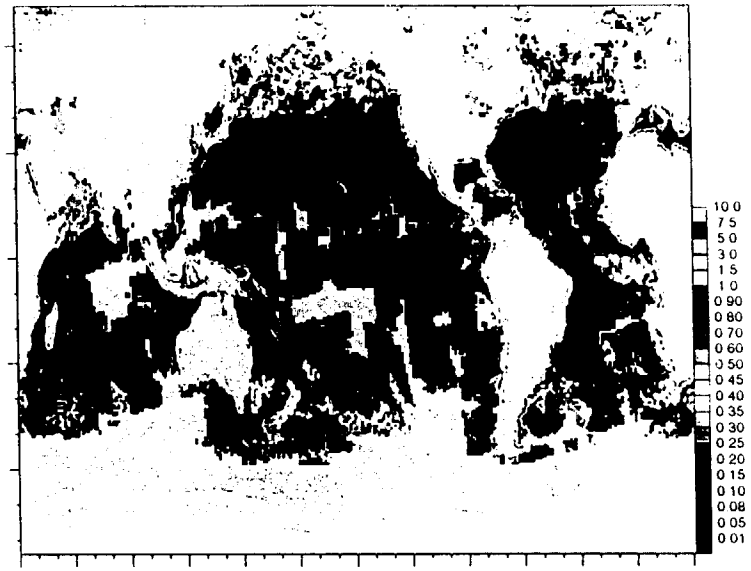

Model Chlorophyll ; December

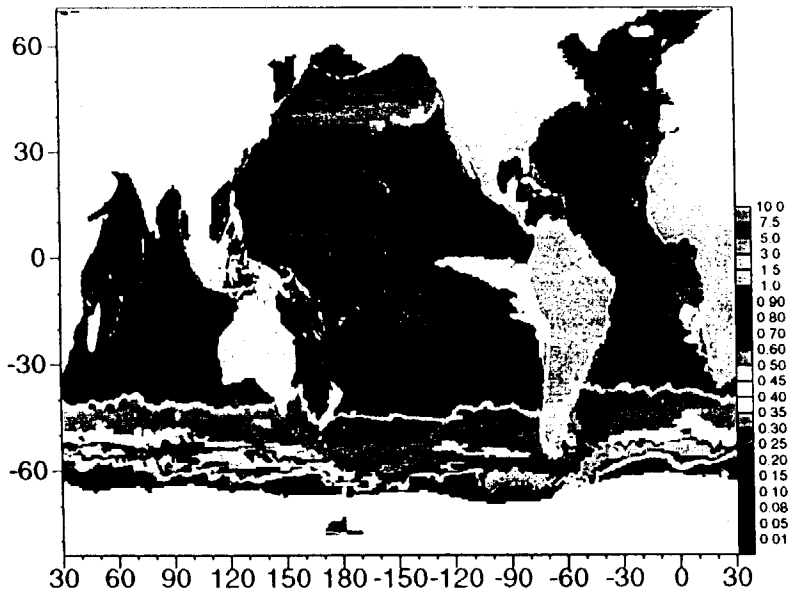

SeaWiFS Chlorophyll; December

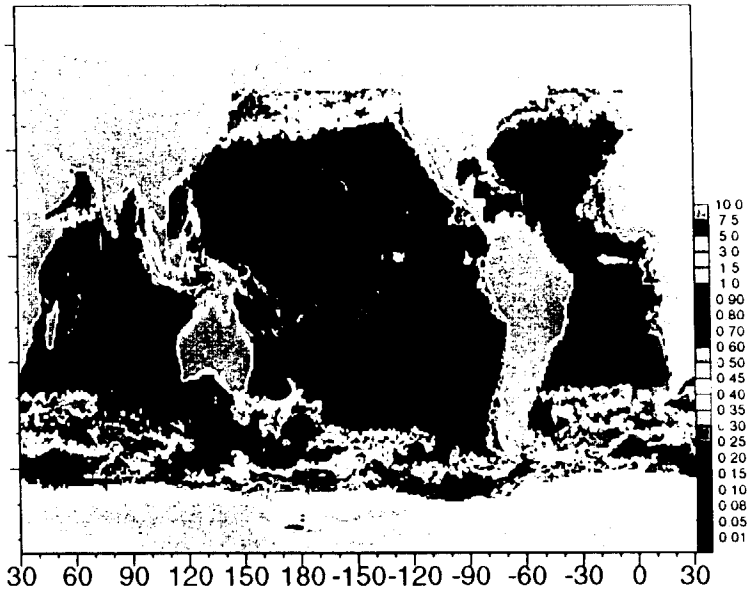

Model Chlorophyll; Summer (Jul-Sep)

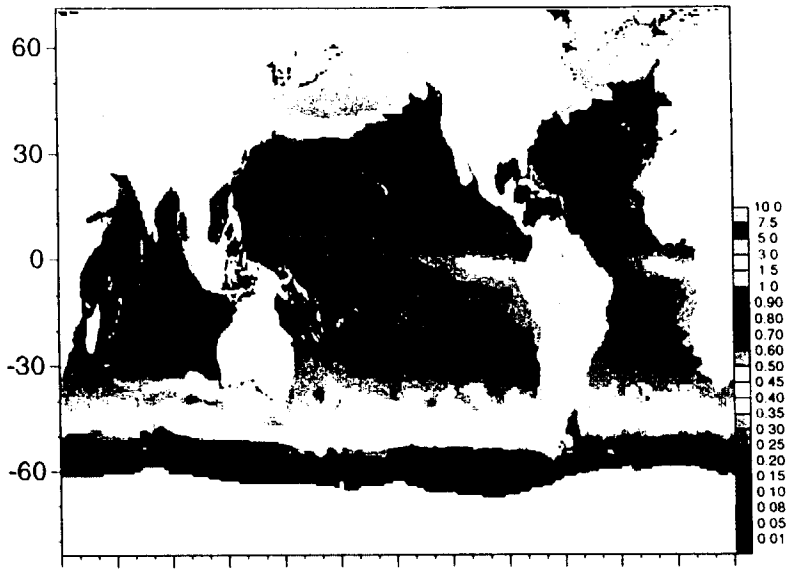

NODC/OCL Chlorophyll; Summer (Jul-Sep)

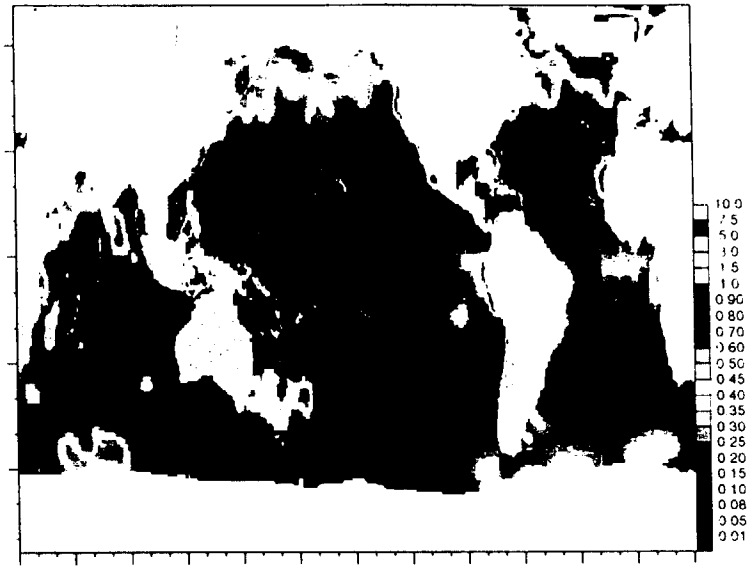

Model Chlorophyll; Autumn (Oct-Dec)

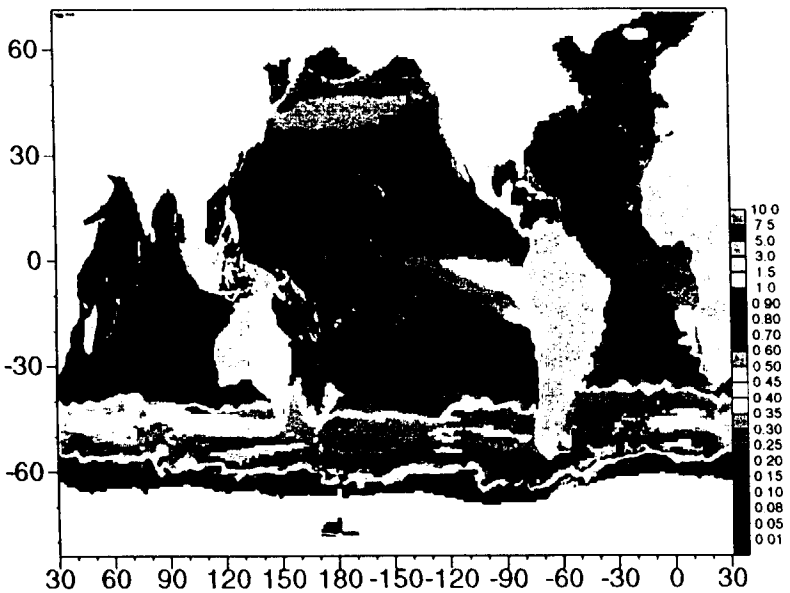

NODC/OCL Chlorophyll; Autumn (Oct-Dec)

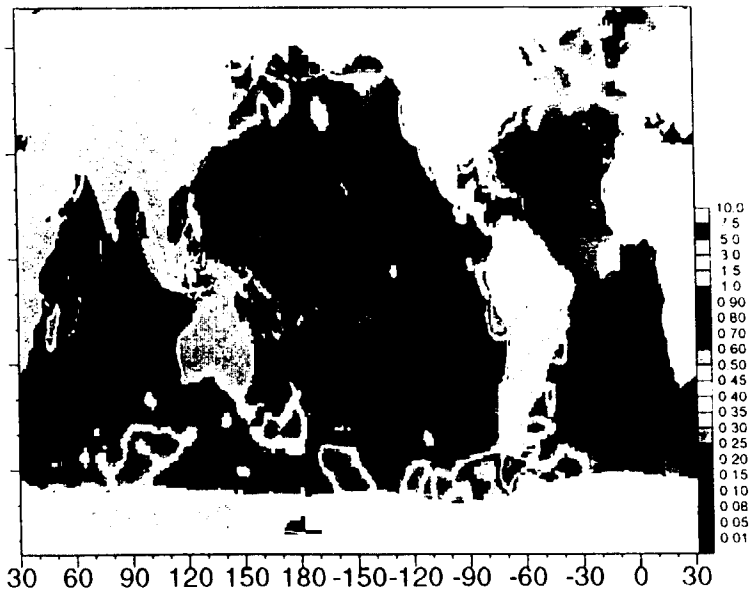

Model Nitrate; Winter (Jan-Mar)

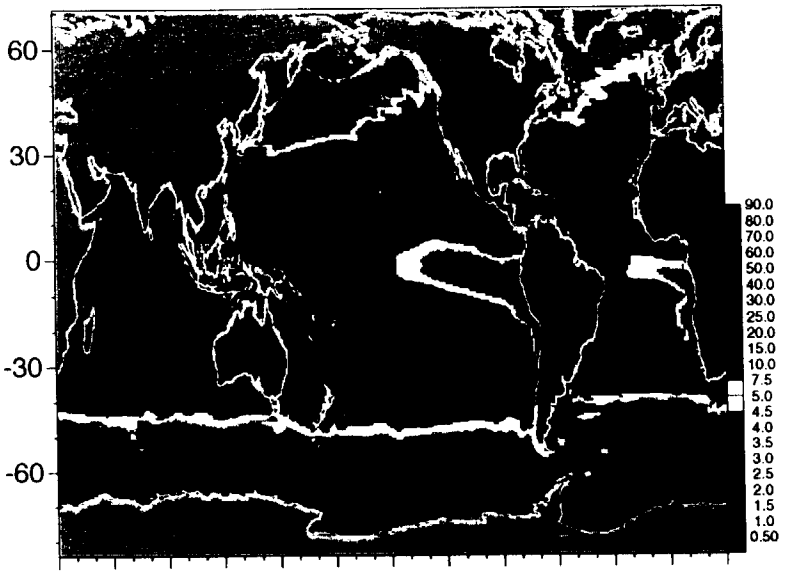

NODC/OCL Nitrate; Winter (Jan-Mar)

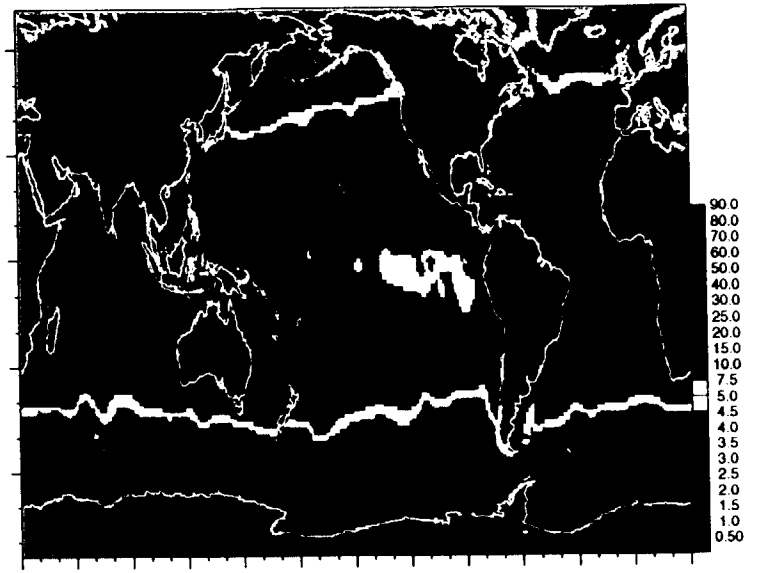

Model Nitrate; Spring (Apr-Jun)

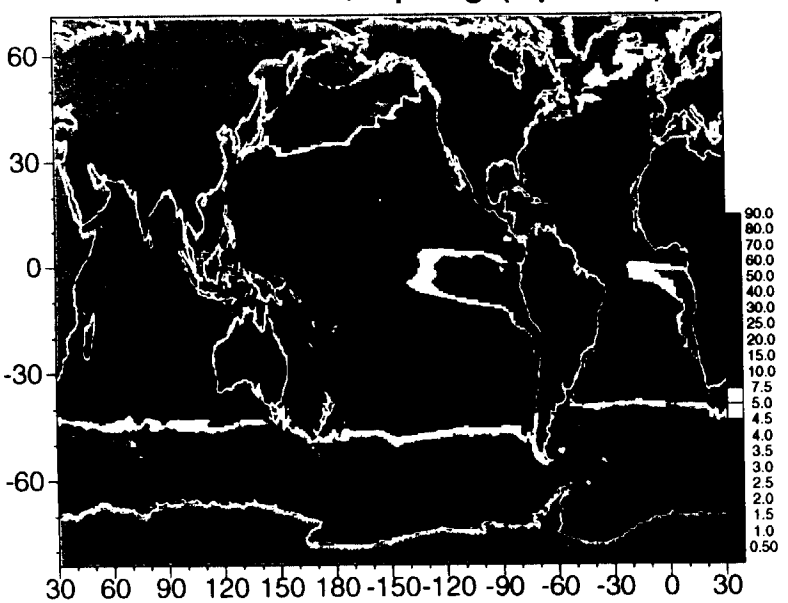

NODC/OCL Nitrate; Spring (Apr-Jun)

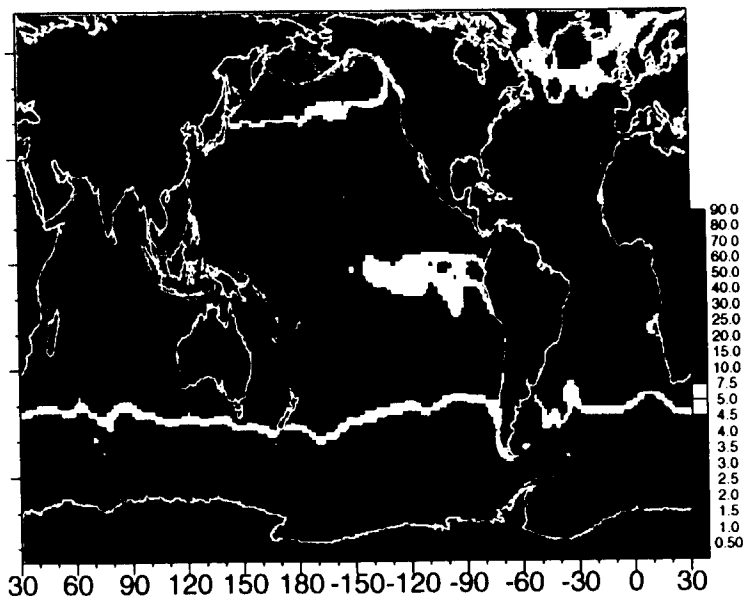

Model Nitrate; Summer (Jul-Sep)

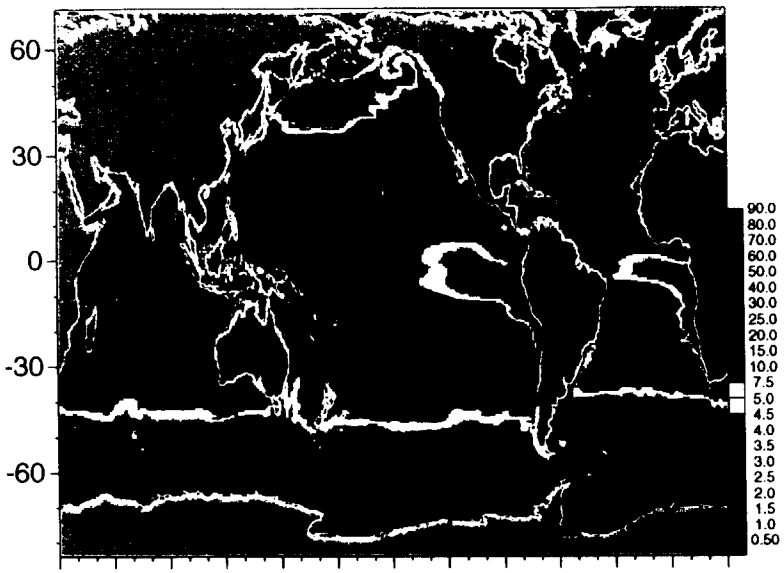

NODC/OCL Nitrate; Summer (Jul-Sep)

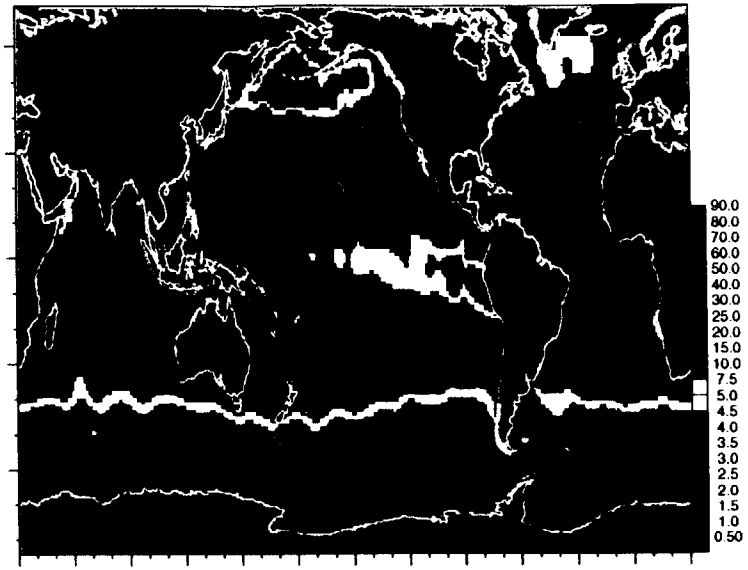

Model Nitrate; Autumn (Oct-Dec)

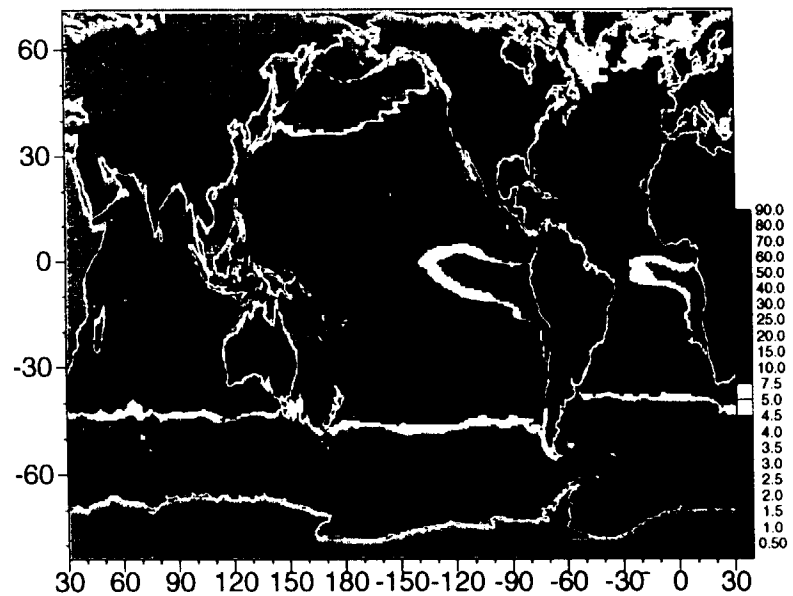

NODC/OCL Nitrate; Autumn (Oct-Dec)